# Column density and temperature effects on narrow resonance structures in atomic photoionization and photoabsorption

J. I. Lo,[1] T. S. Yih,[1] Y. X. Luo,[2] H. S. Fung,[3] Y. Y. Lee,[3] and T. N. Chang[2]
[1]*Department of Physics, National Central University, Chungli 32054, Taiwan, Republic of China*
[2]*Department of Physics and Astronomy, University of Southern California, Los Angeles, California 90089-0484, USA*
[3]*National Synchrotron Radiation Research Center, Hsinchu 30039, Taiwan, Republic of China*
(Received 14 January 2010; published 6 July 2010)

We present a joint experimental and theoretical investigation to resolve the discrepancy in the ratio of relative peak cross sections for narrow atomic resonances among various experimental spectra and also between theory and experiment. Our study includes an effort to measure both the absorption and ionization spectra in a single experimental setup. We also present a careful analysis of the effect on the resonance structure due to the Doppler broadening at finite temperature when the Doppler width is greater than the natural linewidth of the resonance. In addition, we demonstrate that the column density strongly affects not only the absorption structure profile of a narrow atomic resonance but also the ionization spectra measured in an ionization chamber. From the good agreement reported in this article between the observed and the theoretically simulated spectra for the pressure-dependent peak cross sections and the effective asymmetry parameter for the lowest resonance of the He $(1,0)_2^-$ series, we are able to characterize the monochromator (i.e., slit) function of a given light source, including its estimated energy resolution.

DOI: 10.1103/PhysRevA.82.012504 PACS number(s): 32.70.Jz, 32.30.Jc, 32.80.Fb

## I. INTRODUCTION

In spite of the continuous efforts over the past several decades for high resolution measurements with increasingly more sophisticated experimental techniques and large number of high-precision theoretical calculations based on different approaches, substantial discrepancy over the ratio of the relative peak cross sections remains among the observed and calculated results for narrow resonances in atomic photoionization and photoabsorption spectra (see, e.g., Table III of [1] and its discussions for the most often studied He gas at room temperature). The main objective of this article is to investigate the sources of this discrepancy and to propose appropriate procedures to compare the resonance profiles between theoretical and experimental results.

It is generally assumed that the density effect is not significant for photoionization as the interaction zone is usually small (e.g., in a crossed-beam experiment). For photoionization experiments performed in an ionization chamber, on the other hand, the column density for the interaction zone may not be as small. In other words, the total ions or electrons collected in such an experiment could be affected by the column density as the light is attenuated along its interaction path. In fact, we will show in this article that, in principle, if the interaction path is of the order of several cm, the measured ion current would then be affected by the column density, not just for the peak values of the narrow resonance, but also for the background cross sections in the nonresonant region.

The photoabsorption cross section $\sigma^P(E)$ is usually determined by the light attenuation of an incident light of intensity $I_0(E)$ through a gas medium of column density $nl$; that is, it is measured by the Beer-Lambert law,

$$I(E) = I_0(E)e^{-nl\sigma^P(E)}, \tag{1}$$

where $I(E)$ is the attenuated intensity of the transmitted light at photon energy $E$. With a slit function $\mathcal{F}$ centered at the photon energy $E$ and with energy resolution $\Omega$, the incident light intensity $I_0$ and the attenuated light intensity $I$ can be expressed, respectively, as

$$I_0(E;\Omega) = I_0(E)\int \mathcal{F}(E'-E;\Omega)\,dE' \tag{2}$$

and

$$I(E,T;\Omega) = I_0(E)\int \mathcal{F}(E'-E;\Omega)e^{-nl\sigma(E',T)}dE', \tag{3}$$

where $\sigma(E',T)$ is the absolute cross section at an infinite energy resolution and at the temperature $T$ with the slit function given by

$$\mathcal{F}(E'-E;\Omega=0) = \delta(E'-E). \tag{4}$$

Based on Eqs. (1)–(3), the measured resonance structure $\sigma^P(E,T;\Omega)$ in a photoabsorption experiment should be represented by a convoluted spectrum expressed in terms of the true cross section $\sigma$ by an integral in the form of

$$\sigma^P(E,T;\Omega) = -\frac{1}{nl}\ln\left[\int \mathcal{F}(E'-E;\Omega)e^{-nl\sigma(E',T)}dE'\right]. \tag{5}$$

When $nl \to 0$, as expected, the photoabsorption cross section given by Eq. (5) reduces to the usual form for the photoionization cross section (i.e., $\sigma^P \to \sigma^I$), where

$$\sigma^I(E,T;\Omega) = \int \sigma(E',T)\mathcal{F}(E'-E;\Omega)\,dE'. \tag{6}$$

It is known that the measured photoabsorption spectrum for an atomic resonance is significantly affected by the column density $nl$ of the gas medium and the energy resolution $\Omega$ of the experimental monochromator (i.e., slit) function if the width of the resonance $\Gamma$ is substantially smaller than $\Omega$ of the incident light; namely, when $\Gamma/\Omega \ll 1$ [2,3]. This column-density effect is often demonstrated by the change of the measured peak cross section $\sigma_{\max}$ of a narrow resonance as $nl$ varies [3,4].

 

For a light source with relatively high energy resolution, the slit function may be approximated by the combination of a dominating Gaussian distribution function $\mathcal{G}$ at the center and a Lorentzian distribution $\mathcal{L}$ at its tail [2]. It can be expressed by a weighted combination of $\mathcal{G}$ and $\mathcal{L}$:

$$\mathcal{F}(\epsilon;\Omega) = w_g \mathcal{G}(\epsilon;\Omega) + w_\ell \mathcal{L}(\epsilon;\Omega), \tag{7}$$

where $w_g + w_\ell = 1$ and $\mathcal{G}$ and $\mathcal{L}$ are given by

$$\begin{aligned} \mathcal{G}(\epsilon;\Omega) &= \frac{e^{\frac{-\epsilon^2}{\Delta^2}}}{\sqrt{\pi\Delta^2}} \quad \text{and} \\ \mathcal{L}(\epsilon;\Omega) &= \frac{1}{\pi}\frac{\left(\frac{1}{2}\Omega\right)}{\epsilon^2 + \left(\frac{1}{2}\Omega\right)^2}, \end{aligned} \tag{8}$$

respectively, and $\Delta = \Omega/(2\sqrt{\ln 2})$. The energy resolution $\Omega$ is usually measured by the full width at half maximum (FWHM) of the slit function. The rate of change of the peak cross section $\sigma_{\max}$ of the convoluted spectrum is greater for the Gaussian distribution than that of the Lorentzian as $nl$ varies (see, e.g., Figs. 1 and 2 of [4]). It is important to note that, in the absence of a detailed quantitative determination of the three parameters (i.e., $w_g$, $w_l$, and $\Omega$), the convoluted theoretical resonance spectrum for a narrow resonance could be manipulated at will to match the experimental photoabsorption spectrum by adjusting two of these three parameters. As a result, to compare properly the simulated theoretical spectra with the experimentally observed spectra, it is necessary to convolute the theoretical spectra with well characterized $w_g$, $w_l$, and $\Omega$. In principle, the values of $\Omega$ do not have to be the same for the Gaussian and Lorentzian distributions. We could introduce one additional parameter (i.e., a second $\Omega$) to characterize the slit function. However, for simplicity, we choose to employ the same $\Omega$ for Gaussian and Lorentzian distributions in this study. In our analysis, it is relatively straightforward to add the extra parameter if necessary.

In Sec. II, we will discuss in detail the effect of Doppler broadening (i.e., the temperature effect) on the theoretical spectrum. In particular, we will introduce the proper procedure leading to the theoretically simulated spectra. In Sec. III, we present in detail the experimental procedure which measures both the ionization and absorption spectra in one experiment. The use of the ionization chamber in our experiment offers the opportunity for a detailed estimate of the light-attenuation effect on the resonance spectrum as a function of column density along the interaction zone of the ionization chamber. Results and discussions, together with the implication of what we learn in this study, are presented in Sec. IV.

## II. DOPPLER BROADENING

Doppler broadening, which is due to the thermal motion of the gas medium with a molecular (atomic) weight $M$ at a temperature $T$, can be estimated by the expression [5]

$$\Gamma_D = 7.16 \times 10^{-7} E_e \sqrt{\frac{T}{M}}, \tag{9}$$

where $E_e$ is the excitation energy. At a temperature of 298 K, the Doppler broadening is pressure independent and about 0.39 meV for He (with a molecular weight $M = 4$ amu). For a spectral line of the Lorentzian type, the Doppler effect is often taken into account by a slit function described by the Voigt profile [6], which represents a convolution of the Gaussian (Doppler effect) and Lorentzian (natural line) distribution functions.

For a typical isolated autoionization resonance of an atom, its theoretical structure profile, in the absence of Doppler broadening (or at temperature $T = 0$ K) is not of the Lorentzian type. Instead, it is described by the Fano formula [7] in terms of an asymmetry parameter $q$ and the smoothly varying background cross section $\sigma_b$:

$$\sigma(E) = \sigma_b \frac{(q+\epsilon)^2}{1+\epsilon^2}, \tag{10}$$

where $\epsilon = (E - E_r)/(\frac{1}{2}\Gamma)$ is the reduced energy defined in terms of the energy $E_r$ and the natural width $\Gamma$ of the resonance. If the natural linewidth of the resonance is substantially less than the Doppler broadening at finite temperature, instead of the expression given by Eq. (10), the expected resonance structure due to the interaction between the Doppler-shifted photons and the molecules or atoms at a temperature $T$ should be given by

$$\sigma^D(E,T) = \int \sigma(E')\mathcal{P}(E,E';T)\, dE', \tag{11}$$

where

$$\mathcal{P}(E,E';T) = \frac{\exp\left[\frac{-Mc^2(E'-E)^2}{2kTE^2}\right]}{\sqrt{\frac{2\pi kTE^2}{Mc^2}}} \tag{12}$$

is the Doppler-broadening profile due to the Maxwellian velocity distribution at thermal equilibrium [5]. The Doppler width, in terms of Eq. (9), is in fact derived from this Gaussian-type Doppler profile $\mathcal{P}(E,E';T)$; namely,

$$\Gamma_D = 2E\sqrt{\frac{2(\ln 2)kT}{Mc^2}}, \tag{13}$$

where $k$ is Boltzmann's constant.

Since the observed spectra are almost always measured at a temperature $T \gg 0$ K, even under the best experimental conditions such as with the column density $nl \to 0$ and the energy resolution of the slit function of the light source $\Omega \to 0$ (i.e., with extremely high energy resolution), the measured spectrum should be represented by the temperature-dependent resonance structure given by Eq. (11), instead of the usual Fano profile given by Eq. (10). This temperature effect is clearly demonstrated by Fig. 1(a), which compares the theoretically calculated spectrum at zero temperature and the temperature-dependent theoretical spectrum $\sigma^D$ at the temperature $T =$ 298 K for the He $sp23^-$ resonance (i.e., the lowest resonance of the $(1,0)_2^-$ series according to the $(\mathrm{K,T})_\mathrm{N}^\mathrm{A}$ classification [8] or the $(2,1_3)$ line named elsewhere [9]). We shall denote this resonance as the $3^-$ line in all our subsequent discussions. The theoretical spectrum of the $3^-$ line, with an estimated natural width $\Gamma$ close to 0.1 meV and a peak cross section $\sigma_{\max}$ over 20 Mb, was calculated using the B-spline-based configuration interaction (BSCI) method reported in detail elsewhere [10]. Figure 1(b) shows the variation of the peak $\sigma^D$ as $T$ varies. As expected, $\sigma^D_{\max}$ increases to the theoretical value over 20 Mb as the temperature approaches absolute zero.

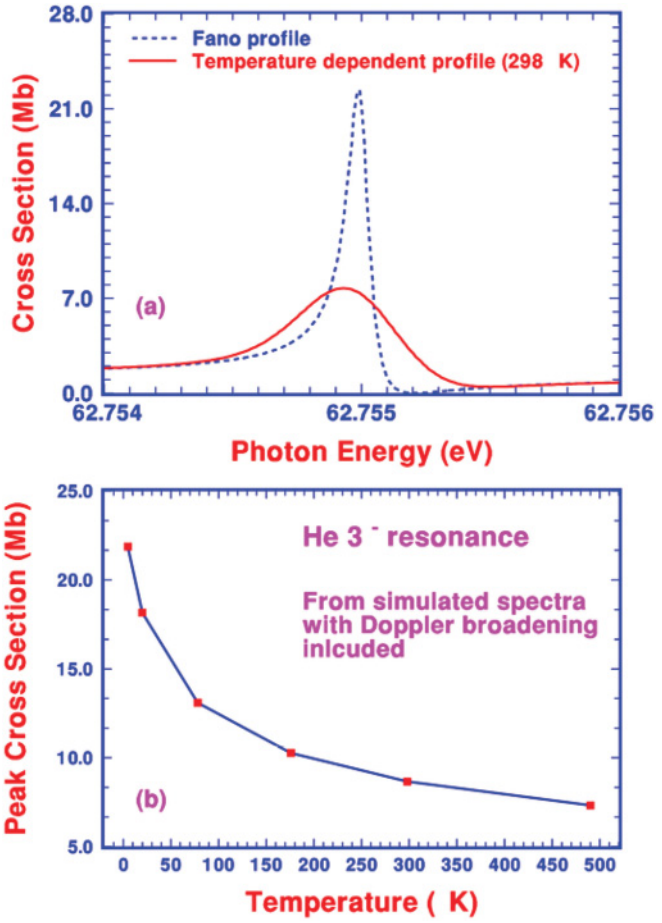


FIG. 1. (Color online) (a) Comparison of the resonance structures of the He $sp23^-$ resonance between the one derived directly from the Fano profile and the simulated temperature-dependent profile with Doppler broadening included and (b) the temperature variation of the peak cross sections from simulated spectra with Doppler broadening included.

The substantial change in the peak cross sections from the theoretical Fano spectrum to the temperature-dependent Doppler spectrum $\sigma^D$ at 298 K shown in Fig. 1 may not account entirely for the discrepancy in the ratio of the peak heights of the narrow resonance structures between experimental and theoretical results discussed earlier. However, one could easily conclude that it is one of the key contributing factors to such discrepancy. Clearly, it is of critical importance for a proper comparison between theory and experiment to employ the temperature-dependent spectrum $\sigma^D$ derived from Eq. (11) in the convolution of the theoretical spectrum following Eqs. (5) and (6) in Sec. I. On the other hand, for a broader resonance of a heavier element, $\Gamma_D$ is usually substantially smaller than the natural width $\Gamma$ and a convolution performed directly from the calculated Fano structure would be a good approximation to the one obtained from the procedure discussed above.

## III. EXPERIMENT AND ATTENUATION EFFECT FOR IONIZATION SPECTRUM

One of the new features in the work reported in this article is the ability to measure both the absorption and ionization spectra in one experiment. Figure 2 shows schematically the experimental setup for the present works. The U9 beamline at the National Synchrotron Radiation Research Center (NSRRC) in Taiwan, with its relatively high spectral resolution estimated at 1.95 meV around 62.755 eV near the He $3^-$ resonance, was chosen as the light source for our experiment. On the front end of the absorption column, shown schematically in Fig. 3, an ionization chamber with a pair of ion-collecting plates of length $\ell = 30$ cm was mounted to measure the photoion current. An Si foil was mounted on the left end of the $L = 1.39$-m light path of the entire chamber. It sustains the pressure difference between the light source and the absorption chamber and, at the same time, blocks the higher order photons generated from the monochromator that might otherwise pass through the absorbing column. After passing through the absorption column, the transmitted light impinged on a sodium salycilate window and was converted into visible fluorescence. This visible fluorescence was in turn detected by a Hamamatsu $1p28A$ PMT. The gas pressure in the absorption column was measured by a pair of MKS Baratrons of 2 Torr and 0.1 Torr full scale, respectively. We are able to control the experimental pressure from slightly below 5 mTorr up to 800 mTorr over two orders of magnitude in column density. Similar experimental procedures detailed elsewhere [11] are employed to measure the absolute photoabsorption cross sections in the present study.

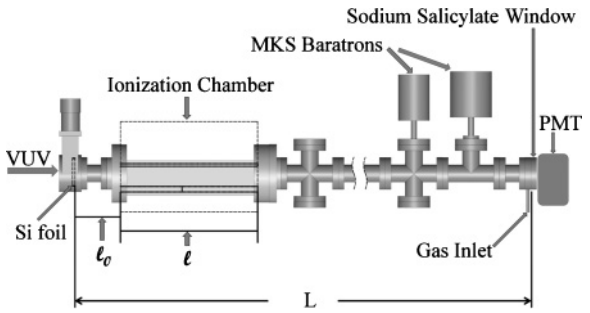


FIG. 2. Schematic of the experimental setup. The ionization chamber is located on the left-hand side of the absorption chamber.

As we pointed out earlier, a proper comparison between the theoretical and experimental spectrum depends critically on the energy resolution $\Omega$ of the slit function. The energy resolution of a light source is often estimated experimentally by its nominal width (i.e., the FWHM value of the spectral line at low pressure). Figure 4 shows the pressure variation of the FWHM values (as defined in Fig. 5) of three simulated theoretical photoabsorption spectra of the He $3^-$ line using a pure Gaussian slit function with $\Omega = 1.90$, 1.95, and 2.0 meV, respectively. The observed FWHM values from our observed photoabsorption spectra at two low pressures confirms the

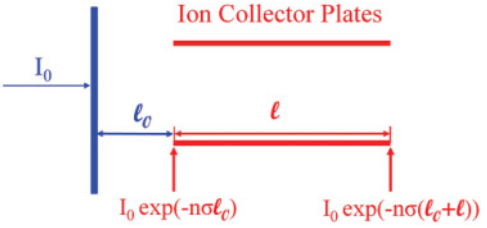


FIG. 3. (Color online) Schematic of the ionization chamber with $\ell_0 = 9$ cm and $\ell = 30$ cm.

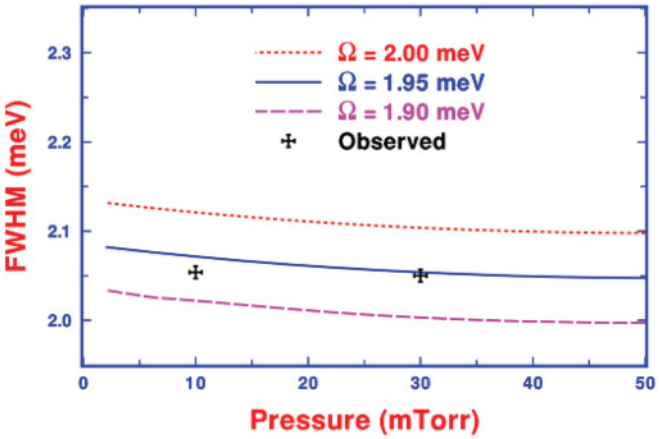


FIG. 4. (Color online) The observed FWHM compared with the ones from the simulated absorption spectra with $\Omega = 1.90$, 1.95, and 2.00 meV at low pressure.

estimated energy resolution close to 1.95 meV for the U9 beamline at the NSRRC.

Since the structure profile of the atomic resonances is not generally symmetric, it is interesting to ask the question that if one could compare the asymmetric structure between theoretical and experimental spectra for a narrow resonance. Ideally, if one could perform the experiment at zero temperature with infinite energy resolution (i.e., at $\Omega = 0$), the theoretically calculated Fano $q$ parameter could be compared directly with the fitted $q$ parameter from the absorbed spectra. Since the experimental conditions are far from optimal, we have chosen instead to characterize the asymmetry of the resonance structure by a modified asymmetry parameter $Q_e$. It measures the ratio of the differences of the maximum and minimum cross sections, respectively, from the background cross section as a function of the column density. This effective asymmetry parameter is defined as

$$Q_e = \sqrt{\frac{\Delta_u}{\Delta_d}} \tag{14}$$

and shown schematically in Fig. 5. Unlike the peak cross section, which could only be compared effectively between

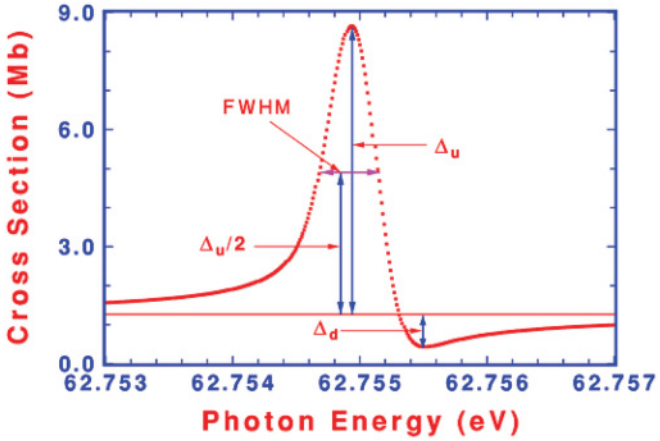


FIG. 5. (Color online) Effective asymmetry parameter $Q_e$ defined by Eq. (14).

theory and experiment for the photoabsorption spectrum with its measured absolute cross sections, $Q_e$ could be compared for both the absorption and ionization spectra.

As the pressure increases, the observed ionization spectrum measured in our experiment is expected to be affected substantially by the light-attenuation effect. Assuming an ionization efficiency $\eta$ for the medium in the chamber, the total ion current collected is given by

$$i(E,T;\Omega) = \eta \Delta I(E,T;\Omega), \tag{15}$$

where the total light attenuation

$$\Delta I(E,T;\Omega) = I_0(E) \int \left[\mathcal{F}(E'-E;\Omega)\left(e^{-n\ell_0\sigma^D(E',T)} - e^{-n(\ell_0+\ell)\sigma^D(E',T)}\right)\right] dE'. \tag{16}$$

The experimental ionization cross section $\sigma_{\text{ion}}(E,T;\Omega)$ may be defined in the usual form:

$$\sigma_{\text{ion}}(E,T;\Omega) = \frac{i(E,T;\Omega)}{\eta n \ell I_0(E;\Omega)}, \tag{17}$$

or

$$\sigma_{\text{ion}}(E,T;\Omega) = \frac{1}{n\ell} \int \left[\mathcal{F}(E'-E;\Omega)\left(e^{-n\ell_0\sigma^D(E',T)} - e^{-n(\ell_0+\ell)\sigma^D(E',T)}\right)\right] dE'. \tag{18}$$

As expected, Eq. (18) reduces to Eq. (6) when both $n$ and $\ell_0$ approach zero. Of course, in practice, it is the total ion current that is measured experimentally.

Equation (18) shows clearly that the measured cross sections $\sigma_{\text{ion}}$ are affected by the light attenuation as column density of the medium varies. In fact, even with a near constant $\sigma^D$, $\sigma_{\text{ion}}$ will vary as a function of column density. This could be seen analytically by considering the slow varying $\sigma_{\text{ion}}$ or when $\frac{d\sigma^D}{dE} \to 0$ from Eq. (18). Since $\sigma^D$ is approximately a constant, the integration over $E'$ will only include the slit function $\mathcal{F}(E'-E;\Omega)$, and $\sigma_{\text{ion}}$ reduces to

$$\sigma_{\text{ion}} = \frac{1}{n\ell}\left(e^{-n\ell_0\sigma^D} - e^{-n(\ell_0+\ell)\sigma^D}\right). \tag{19}$$

The resulting Eq. (19) can be expanded approximately in terms of a polynomial of $x_0 = n\ell_0\sigma^D$; namely,

$$\sigma_{\text{ion}} = \sigma^D\left[1 - \left(1+\frac{\zeta}{2}\right)x_0 + \frac{1}{2}\left(1+\zeta+\frac{\zeta^2}{3}\right)x_0^2 + \cdots\right], \tag{20}$$

where $\zeta = \frac{\ell}{\ell_0}$. Evidently, $\sigma_{\text{ion}}$ will be modified as the column density increases due to the presence of the additional terms in Eq. (20).

In addition to the attenuation effect, the measured widths of the observed structures will also be affected by the collision-induced excitation or deexcitation of the target atoms (i.e., pressure broadening) as pressure increases. It is well known that, qualitatively, the pressure broadening $\Gamma_P(P)$ is proportional to the pressure $P$ (or column density) [12]:

$$\Gamma_P(P) = \alpha P, \tag{21}$$

where $\alpha$ is the pressure-broadening coefficient.

Experimentally, as pressure increases, the increase in the measured width $\Delta W_{\text{expt}}$ can be attributed to the pressure broadening $\Gamma_P$ and the column density effect $\Delta\Gamma_c$, that is,

$$\Delta W_{\text{expt}}(P) = \Gamma_P + \Delta\Gamma_c. \tag{22}$$

With $\Delta\Gamma_c$ determined by a procedure outlined below, Eq. (22) suggests that one will be able to estimate the pressure broadening $\Gamma_P$ if the increase in the experimental spectral widths $\Delta W_{\text{expt}}(P)$ could be measured with sufficiently high accuracy.

The increase in width $\Delta\Gamma_c$ due to the column density effect could be determined from the simulated theoretical spectra calculated with Eqs. (5) and (18) for absorption and ionization, respectively. We should note again that the temperature-dependent spectrum $\sigma^D$ at 298 K should be the one (instead of the theoretical Fano spectrum) that is applied in the calculation of the simulated spectra. To estimate the effect due to the light attenuation as $n$ increases, we first determine the FWHM width $\Gamma_c(n_0)$ from the simulated theoretical spectrum at the lowest experimental pressure $P_0$, where $n_0$ is the corresponding number density. For the ionization measurement, with $\ell = 30$ cm and $\ell_0 = 9$ cm, the ionization chamber operates in the present experiment has a value of $n\ell\sigma_{\text{peak}}$ around 0.12 for the He $3^-$ line at the lowest pressure $P_0 = 5$ mTorr. This lowest pressure is chosen to assure a near-zero attenuation effect at $n_0$. We then determine the FWHM width $\Gamma_c(n)$ at a number of higher densities $n$ (or pressures) using Eq. (18). The contribution to the increase in width due to the light attenuation at different column density $n\ell$ is then estimated by the difference $\Delta\Gamma_c = \Gamma_c(n) - \Gamma_c(n_0)$. The same procedure could also be applied to determine $\Delta\Gamma_c$ from the absorption measurement.

## IV. RESULTS AND DISCUSSIONS

Figure 6 compares the observed spectra with the simulated theoretical spectra at pressure $P = 50$ mTorr for the He $3^-$ line. We obtain the best agreement between theory and experiment (as shown) with a slit function dominated by the Gaussian distribution at $w_g = 0.8$. For the ionization spectra, the observed relative cross sections are normalized against the simulated theoretical spectra. The overall agreement between theory and experiment is very good. Figure 7 shows the substantial column density effect to the resonance structures as the pressure increases from 5 to 200 mTorr. For the absorption spectra, the background cross section stays the same while the peak cross section decreases as pressure increases. For the ionization spectra, as expected, both background and peak cross sections decrease as pressure increases. Before we present in detail the additional results, we should point out that the most critical test for what we report in this article is the good agreement between theory and experiment for all three pressure-dependent observables; namely, the absolute peak cross section from the absorption spectrum and the two effective asymmetry parameters $Q_e$ from the absorption and ionization spectra, respectively.

Figure 8 compares the measured absolute photoabsorption peak cross sections and the ones from the simulated spectra. The peak cross sections obtained from the simulated spectra convoluted with the temperature-dependent Doppler spectrum

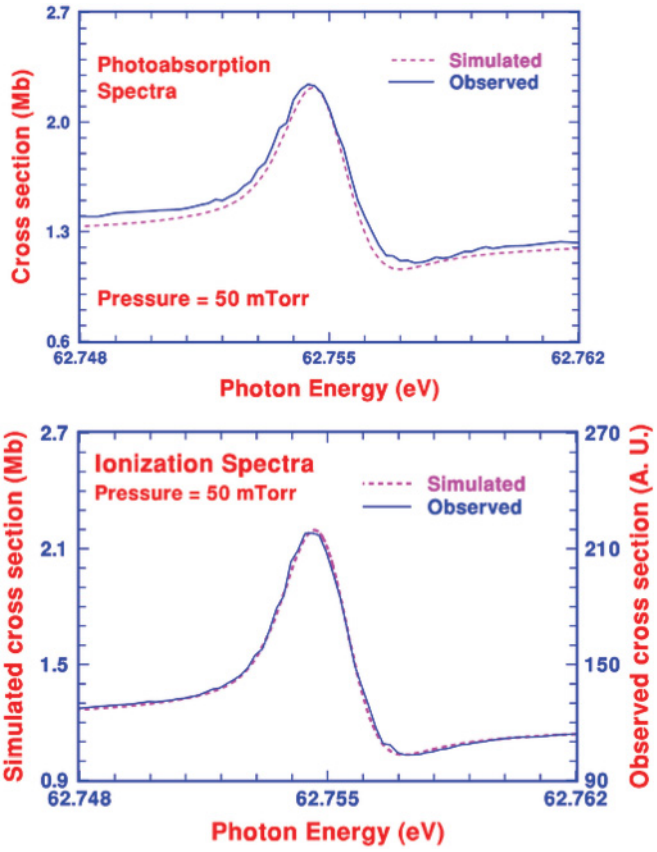


FIG. 6. (Color online) Comparison between the observed and simulated spectra at $P = 50$ mTorr.

are in much closer agreement with the measured ones than the peak cross sections from the simulated spectra convoluted directly with the Fano spectrum. We have also carried out the calculation by increasing arbitrarily the $q$ value by about 20% to examine how the variation in the theoretical $\sigma_{\text{max}}$ may affect the simulated peak cross sections as pressure varies. Our results show an increase in the simulated $\sigma_{\text{max}}$ by as much as 15% at low pressures with, as expected, little effect at higher pressures; that is, leading to a pressure dependence of $\sigma_{\text{max}}$ that deviates substantially from the observed peak cross sections.

Since the simulated spectra do not include the effect due to the pressure broadening, the small difference at higher pressure between the simulated and the observed results could be attributed qualitatively to the collision-induced excitation or deexcitation of the target atoms, which reduces the number density and thus less light attenuation and smaller observed peak cross section. We also note from Fig. 7 that, as pressure increases, the peak cross section decreases at a rate greater than that of the minimum cross section. As a result, one should expect that the effective asymmetry parameter $Q_e$, as defined in Sec. III, should decrease as pressure increases. Indeed, Fig. 9 shows such a decrease for the photoabsorption as well as for the ionization. The agreement between the observed $Q_e$ and the ones obtained from the simulated spectra are very good. We also include in Fig. 9 the effective $Q_e$ obtained from the simulated spectra convoluted directly from the theoretical Fano spectrum. The small difference at higher pressure between the simulated and observed results, again,

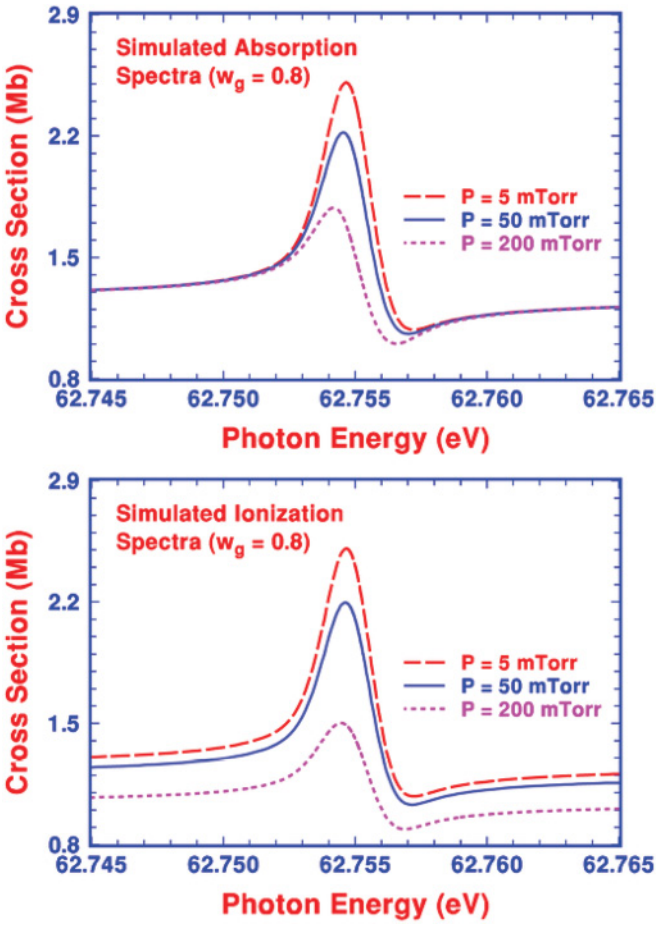


FIG. 7. (Color online) Simulated absorption and ionization spectra at $P = 5$, 50, and 200 mTorr.

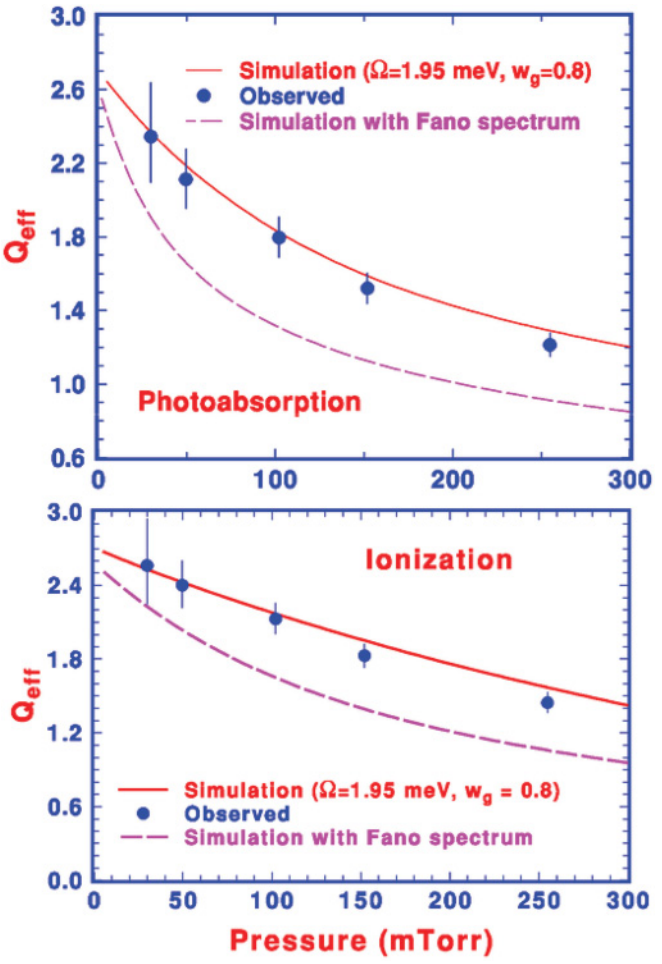


FIG. 9. (Color online) The effective asymmetry parameters $Q_e$ as functions of pressure from the observed and simulated absorption or ionization spectra. $Q_e$ from the simulated spectra convoluted directly with Fano spectrum are also shown for comparison.

could be attributed to the neglect of the effect due to the pressure broadening in the simulated spectra as we discussed earlier. From the comparison of the three key observables shown in Figs. 8 and 9, we conclude that it is necessary to determine first the relative values of the energy resolution $\Omega$ of the slit function, the Doppler width $\Gamma_D$ at temperature $T$, and the estimated natural width $\Gamma$ of the resonance line, before one proceeds to convolute the theoretically calculated spectra for a proper comparison with the experimentally observed spectra.

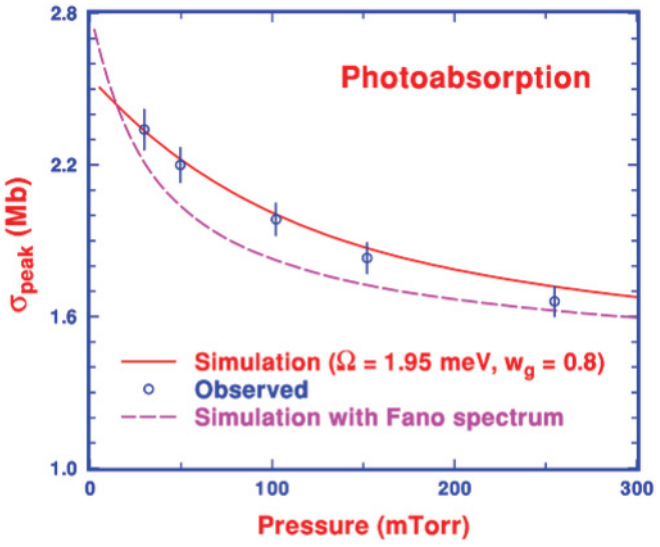


FIG. 8. (Color online) The peak cross sections as functions of pressure from the observed and simulated absorption spectra. The results from the simulated spectra convoluted directly with the Fano spectrum are also shown for comparison.

Figure 10 shows the pressure variation of the FWHM from the absorption and ionization spectra. At low pressure (e.g., below 50 mTorr), the increase in FWHM, [i.e., $\Delta W_{\text{expt}}$ from Eq. (22)], is minimal since both pressure broadening and column density effect due to light attenuation are expected to be small. The FWHM derived from the simulated spectra, which include the column density effect due to light attenuation, indeed increase as pressure increases. The experimental error bars shown are significantly larger than those shown in Fig. 9 since we include in the displayed errors the maximum uncertainty in monochromator scan steps of 0.1 meV. The actual error should be smaller than what is shown. The difference between the observed and the simulated FWHM represents the contribution to the width from the pressure broadening, as we discussed in Sec. IV.

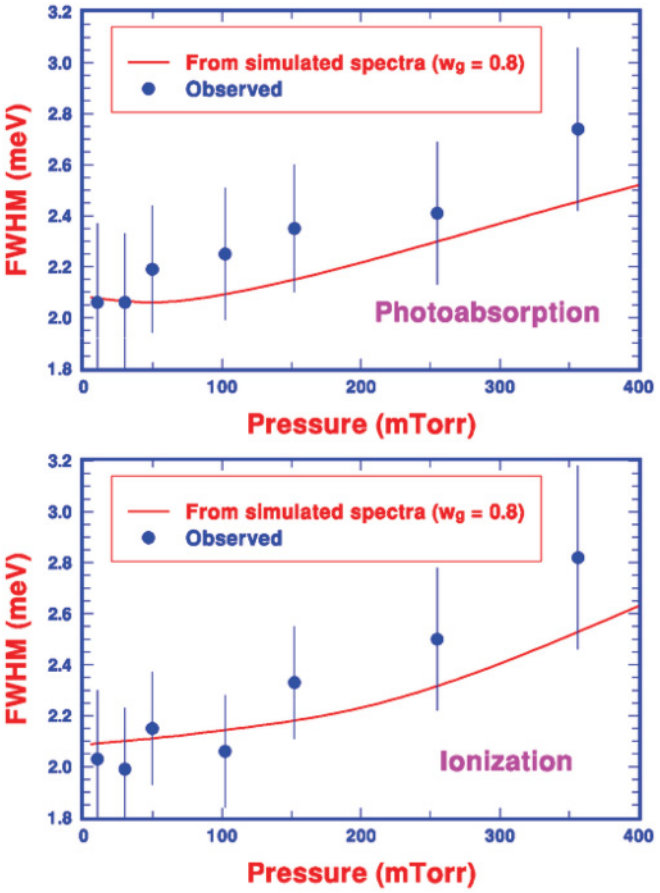


FIG. 10. (Color online) The pressure-dependent FWHM derived from the observed and simulated absorption or ionization spectra. The difference in FWHM between the observed and calculated spectra at higher pressure due to the pressure broadening is expected to increase linearly as a function of the pressure.

At an experimental energy resolution close to 1.95 meV, which is comparable to the measured FWHM between 2 and 3 meV, the seemingly good agreement between the simulated and measured absorption resonance structures at 50 mTorr, shown in Fig. 6, has in fact led to a large difference in FWHM shown in Fig. 10. Following the procedure outlined in Sec. IV, Fig. 11 presents an order-of-magnitude estimate of the pressure broadening coefficient $\alpha$, given by the slope of the straight line derived from the pressure variation of $\Gamma_P = \Delta W_{\text{expt}}(P) - \Delta\Gamma_c$. From the experimental uncertainties shown in Fig. 10, clearly, this estimated pressure broadening

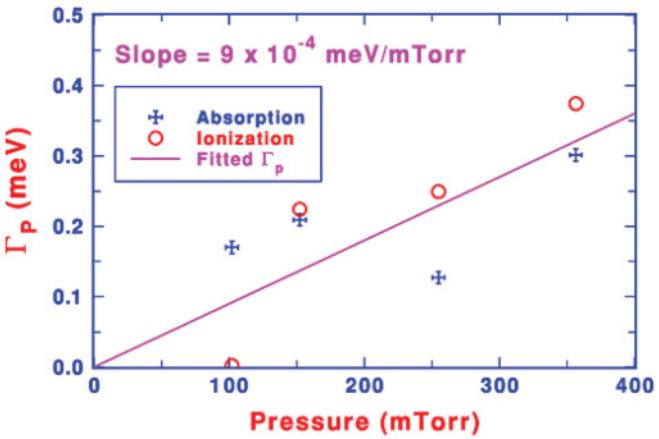


FIG. 11. (Color online) Estimated pressure broadening coefficient (i.e., the slope of the straight line) following the procedure outlined in Sec. IV.

coefficient is far from satisfactory. In spite of the intrinsic challenge that the measured FWHM will always differ only slightly from the energy resolution of the slit function, our result, nevertheless, suggests a possible procedure that could lead to a more accurate determination of the pressure broadening coefficient, given more beam time and better statistics in the data collection.

The analysis presented in this article offers a possible resolution of the discrepancy in peak cross sections of the narrow resonances between theory and experiment in atomic photoabsorption and photoionization. The narrow doubly excited He resonance structures, with the help of high-resolution experimental measurements and precision theoretical calculations, may serve as a good candidate to calibrate in detail the slit function of the light source following the joint theoretical and experimental procedure proposed in this article. More reliable measurement of the FWHM of the resonance structure could also lead to an accurate determination of the pressure broadening coefficient, which is not readily available either theoretically or experimentally.

## ACKNOWLEDGMENTS

This work was supported by the National Science Council in Taiwan under the grant numbers NSC 98-2119-M-007-001 and 96-2112-M-008-010-MY3.

[1] K. C. Prince, R. Richter, M. de Simone, M. Alagia, and M. Coreno, Phys. Rev. A **68**, 044701 (2003).
[2] T. K. Fang and T. N. Chang, Phys. Rev. A **57**, 4407 (1998).
[3] R. D. Hudson and V. L. Carter, J. Opt. Soc. Am. **58**, 227 (1968); W. F. Chan, G. Cooper, and C. E. Brion, Phys. Rev. A **44**, 186 (1991).
[4] T. N. Chang, Y. X. Luo, H. S. Fung, and T. S. Yih, J. Chin. Chem. Soc. **48**, 347 (2001).
[5] W. Demtröder, *Laser Spectroscopy* (Springer-Verlag, Berlin, 1996), p. 68.
[6] M. Mizushima, *Quantum Mechanics of Atomic Spectra and Atomic Structure* (W. A. Benjamin, New York, 1970), p. 103; R. D. Cowan, *Theory of Atomic Structure and Spectra* (University of California Press, Berkeley, 1981), p. 20; W. Demtröder, *Laser Spectroscopy* (Springer-Verlag, Berlin, 1996), p. 71.
[7] U. Fano, Phys. Rev. **124**, 1866 (1961).

[8] C. D. Lin, Phys. Rev. A **29**, 1019 (1984); D. R. Herrick and O. Sinanoğlu, *ibid.* **11**, 97 (1975).

[9] K. Schulz, G. Kaindl, M. Domke, J. D. Bozek, P. A. Heimann, A. S. Schlachter, and J. M. Rost, Phys. Rev. Lett. **77**, 3086 (1996); M. Domke, K. Schulz, G. Remmers, and G. Kaindl, Phys. Rev. A **53**, 1424 (1996).

[10] T. N. Chang, Phys. Rev. A **47**, 3441 (1993); *Many-Body Theory of Atomic Structure and Photoionization* (World Scientific, Singapore, 1993), p. 213.

[11] H. S. Fung, C. C. Chu, S. J. Hsu, H. H. Wu, and T. S. Yih, Rev. Sci. Instrum. **71**, 1564 (2000); H. S. Fung and T. S. Yih, Nucl. Phys. A **684**, 696c (2001).

[12] W. Demtröder, *Laser Spectroscopy* (Springer-Verlag, Berlin, 1996), p. 74.